Criticality of Low-Energy Protons in Single-Event Effects Testing of Highly-Scaled Technologies

Jonathan A. Pellish, *Member, IEEE*, Paul W. Marshall, *Fellow, IEEE*,
Kenneth P. Rodbell, *Senior Member, IEEE*, Michael S. Gordon, *Senior Member, IEEE*,
Kenneth A. LaBel, *Member, IEEE*, James R. Schwank, *Fellow, IEEE*,
Nathaniel A. Dodds, *Member, IEEE*, Carlos M. Castaneda, *Member, IEEE*,
Melanie D. Berg, *Member, IEEE*, Hak S. Kim, Anthony M. Phan, and Christina M. Seidleck

***Abstract*—We report low-energy proton and low-energy alpha particle SEE data on a 32 nm SOI CMOS SRAM that demonstrates the criticality of using low-energy protons for SEE testing of highly-scaled technologies. Low-energy protons produced a significantly higher fraction of multi-bit upsets relative to single-bit upsets when compared to similar alpha particle data. This difference highlights the importance of performing hardness assurance testing with protons that include energy distribution components below 2 MeV. The importance of low-energy protons to system-level single-event performance is based on the technology under investigation as well as the target radiation environment.**

***Index Terms*—alpha particle radiation effects, proton radiation effects, radiation hardness assurance testing, silicon-on-insulator technology, single-event upset.**

I. Introduction

In 2007, K. P. Rodbell *et al.* demonstrated that low-energy protons, those with less than 2 MeV of kinetic energy, could cause single-event upsets (SEUs) in 65 nm silicon-on-insulator (SOI) complementary metal oxide semiconductor (CMOS) latches and static random access memory (SRAM) cells [1]. They alleged that the protons caused SEUs via primary particle direct ionization. Work transitioned to more applied efforts [2-5] and important follow-on studies at additional CMOS process nodes, including 90, 45, 32, and 28 nm [6-11]. Our work here focuses on the need to revisit and refine several previous radiation hardness assurance (RHA) postulates related to low-energy proton effects.

Almost as soon as low-energy proton single-event effects (SEE) were presented by Rodbell *et al.* [1], the radiation effects community started trying to figure out whether this potential threat was a concern for proton-dominated trajectories and orbits. Initial information was presented by Heidel *et al.* [6] and was expanded by Sierawski *et al.* [2], Cannon *et al.* [4], and Hubert *et al.* [3]. A lot of this debate centered on whether experimenters had to use degraded beams of low-energy protons with significant straggle or, since primary particle direct ionization was the assumed mechanism, whether a surrogate beam of alpha particles or other low-linear energy transfer (LET) light ions could be utilized to simulate the low-energy protons' electronic LET and thus the correct proportion of SEUs with enough fidelity to make accurate event rate calculations. For clarity, we will use the term "light ions" to refer to heavy ions with $1 < Z \leq 10$ throughout the text. Using the higher energy beams was desirable since many systematic errors could be eliminated with increased particle range and lower straggle.

Based on recent data collection, we show that in most cases it is not advisable to use alpha particles, or other high-energy light ions, to circumvent the need to conduct SEE characterization testing with low-energy protons. This is especially true for components or environments where the low-energy proton event rate contribution could be significant. Sierawski *et al.* [2], Cannon *et al.* [4], and Dodds *et al.* [12] showed there are instances where low-energy proton SEE could significantly contribute to a component's single-event radiation response, as indicated in [2, 12] for 65 nm bulk and SOI CMOS SRAMs. A higher inclination and/or higher altitude trajectory could increase these event rates substantially.

The work presented here synthesizes information from previous studies and focuses on two areas: 1) complications arising from the use of high-energy light ions to screen for and

Manuscript received 11 July 2014. This work was supported in part by the NASA Electronic Parts and Packaging (NEPP) Program, the Defense Threat Reduction Agency (DTRA) under IACRO DTRA10027-8002 to NASA, the National Reconnaissance Office, and the Laboratory Directed Research and Development program at Sandia National Laboratories, a multi-program laboratory operated by Sandia Corporation, a Lockheed Martin Company, for the United States Department of Energy, under contract DE-AC04-94AL85000.

J. A. Pellish and K. A. LaBel are with the NASA Goddard Space Flight Center, 8800 Greenbelt RD, Greenbelt, MD 20771 USA. Corresponding author contact – phone: 301.286.8046; email: jonathan.pellish@nasa.gov.

P. W. Marshall is a NASA consultant, Brookneal, VA 24528 USA.

K. P. Rodbell and M. S. Gordon are with the IBM T. J. Watson Research Center, Yorktown Heights, NY 10598 USA.

J. R. Schwank and N. A. Dodds are with Sandia National Laboratories, Albuquerque, NM 87185 USA.

C. M. Castaneda is with the Crocker Nuclear Laboratory at the University of California/Davis, Davis, CA 95616 USA.

M. D. Berg, H. S. Kim, A. M. Phan, and C. M. Seidleck are with ASRC Federal Space & Defense in support of the NASA Goddard Space Flight Center, Greenbelt, MD 20771 USA.

quantify low-energy proton effects, and 2) the importance of low-energy proton-induced multi-bit upsets (MBUs). The use of high-energy light ions, like alpha particles, as a low-energy proton surrogate was first suggested by Sierawski *et al.* [2]. Low-energy proton MBUs were first discussed by Heidel *et al.* [8]. Their data analysis on a 45 nm SOI CMOS SRAM did not elaborate much beyond the presentation of the increased double-bit upset (DBU) cross section at low proton energies, granting the possibility of a wide range of interpretations. The authors note that our community usually imputes different meanings to MBUs and multi-cell upsets (MCUs). MBUs happen when a single particle causes more than one data error bit in a single data word. MCUs are more than one physically-adjacent data error that may or may not be in the same data word. Our analysis only looks at physically-adjacent multi-bit errors, which are MCUs, so we will refer to them as MCUs throughout the rest of this paper.

Table I: Basic Configuration of CNL SEE Beam Line

Beam Line Element	Thickness (μm)
Tantalum scattering foil	6.35
Collimator (0.95 cm diameter)	N/A
Phosphorus Screen	N/A
Defining Collimator (6.0 cm diameter)	N/A
Aluminum SEEM* foils	6.35
User-selected degraders (Mylar and/or aluminum)	0 – 150
Kapton exit window	127
Air gap	5×10^4
Silicon substrate of DUT	70 – 100

*Secondary electron emission monitor (SEEM)

The 32 nm SOI CMOS SRAM data we present here demonstrates that a given fluence of low-energy protons will result in a much larger fraction of DBUs and higher multiplicity events than an equivalent fluence of alpha particles for all test energies. This fact calls into question the original suggestion that primary particle electronic d*E*/d*x* alone can account for the increased proton event cross sections at low energy, thereby invalidating the hypothesis that high-energy light ions can be used as a low-energy proton substitute. While the physically-adjacent SRAM DBUs could be mitigated in a commercial or radiation-hardened by design (RHBD) device via a different bit cell arrangement and the use of error detection and correction (EDAC), these events are important because they allow us to spatially correlate significant energy deposition events because critical charge preferentially samples these instances. Furthermore, higher multiplicity events like three- or four-bit upsets may not be able to be corrected. These findings have important implications for ultra-deep submicron processes and extend beyond the effects we observed in this SRAM test vehicle. RHBD techniques, such as stacked storage elements and dual interlocked cells (DICE), cannot ignore these proton-specific effects and should be tested with low-energy protons rather than with high-energy light ions alone.

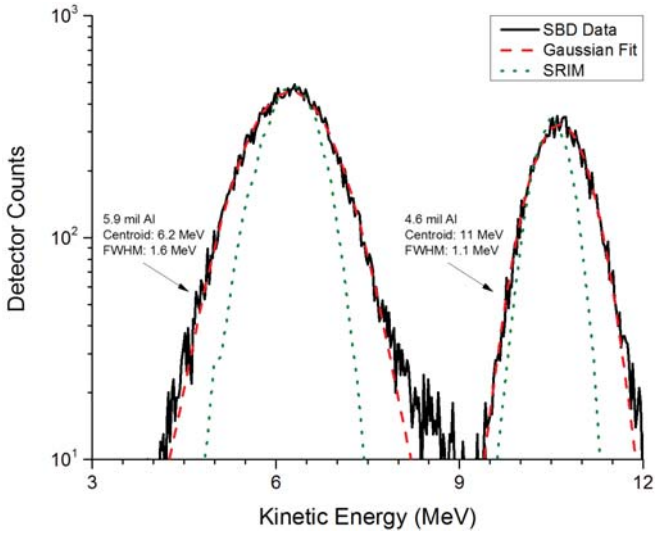

Fig. 1: Degraded 30 MeV alpha particle energy spectra captured with a calibrated silicon surface barrier detector (SBD) along with Gaussian data fits and SRIM simulations. All data were taken with a 2 cm air gap. The text to the left of the curves refers to the degrader thickness and the major Gaussian fit parameters. These energy spectra do not include transport through DUT's silicon substrate.

II. Experimental Details

A. Experimental Facility and Device Under Test

We used the Crocker Nuclear Laboratory (CNL) at the University of California/Davis for all of the proton and alpha particle measurements. Irradiations were conducted in air under room temperature conditions at normal incidence with a 5 cm air gap between the end of the beam line and the surface of the device under test (DUT). A description of the beam line elements and their thicknesses is shown in Table I. The beam was collimated to a diameter of 1.6 cm. CNL accelerates ions using a 76-in isochronous cyclotron to accelerate its ion beams. The alpha particle beams were tuned to an initial kinetic energy of 30 MeV and the proton beams were delivered with either 64 or 6.5 MeV of kinetic energy. To produce the low-energy proton beam, CNL accelerates H_2^+ (ionized molecular hydrogen) to 13 MeV and then breaks the molecule into two protons by passing it through the upstream tantalum scattering foil; each proton receives half of the original kinetic energy. The tuned energies of these proton and alpha particle beams can then be degraded using a LabVIEW™-controlled degrader box bolted to the end of the beam line, which provides a wide range of aluminum and polyethylene terephthalate (Mylar) foil thicknesses. Additional details of this beam line and the degrader foils were previously described in [13, 14].

To aid data analysis and transport simulations, we measured and simulated the energy spectra of several foil degrader combinations for both protons and alpha particles. These alpha particle and proton energy spectra data are used to calibrate subsequent radiation transport simulations so that beam line degrader combinations can be converted to average particle kinetic energies. Fig. 1 shows two degraded 30 MeV

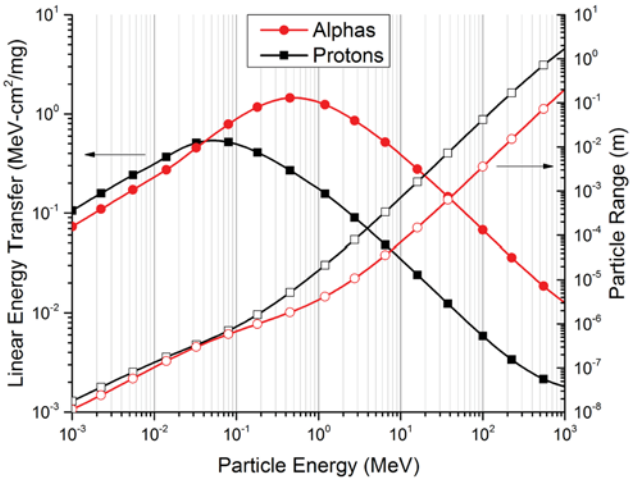

Fig. 2: The plot shows SRIM (v2013) stopping and range calculations for both protons and alpha particles ranging from 1 keV to 1 GeV. There are portions of the energy range where protons and alpha particles have similar LET and range characteristics. All values are relative to silicon. These are lookup table results as opposed to Monte Carlo results from a TRIM (Transport of Ions in Matter) simulation. Data symbols have been made sparse.

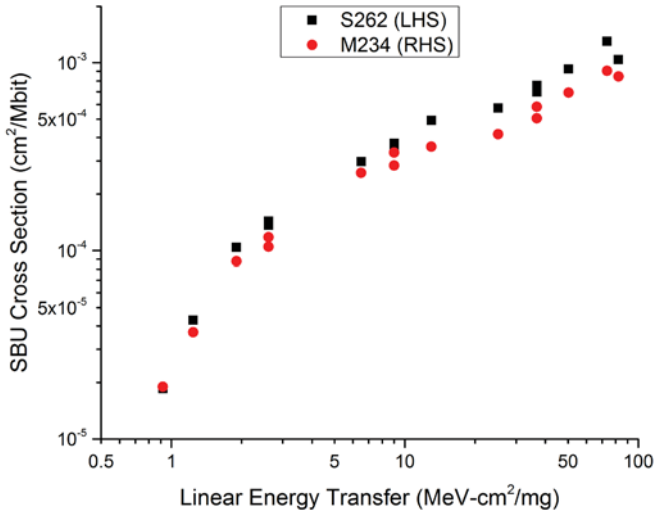

Fig. 3: Heavy ion SBU data gathered at the TAMU cyclotron facility. These data represent physical checkerboard data for both halves of the SRAM DUT, which was biased with an array voltage of 1.05 V (nominal). These data include irradiations with N, Ne, Ar, Kr, and Xe ions at 25 MeV/amu. The S262 bit cells have slightly larger cross sections than the M234 bit cells, which is clearly visible in the data above 1 MeV-cm^2/mg. This plot includes effective LET.

alpha particle energy spectra and their associated Gaussian peak fits and matching SRIM [15] transport simulations. Measuring these energy spectra is a critical step in validating experimental results since the particle energy changes rapidly as it passes through the DUT, invalidating average quantities like LET. Previous work [2, 14, 16] described why tools like SRIM can produce discrepancies with experimental data, as seen in Fig. 1. Similar types of measured proton energy spectra at CNL have been discussed previously [14] and the proton energy spectra we measured during this test campaign compare well, so we feel there is little to be gained by presenting them.

For reference, we have included the proton and alpha particle LETs and ranges for silicon in Fig. 2. It is important to note that the Bragg peaks, where the energy deposition per unit length is maximized, occurs at approximately 0.05 MeV for protons and at 0.5 MeV for alpha particles, after which point each particle's range is no more than a few microns. Below 0.1 MeV, the particle ranges are much less than 1 µm. Because the particle ranges are so short in this regime, straggle becomes important and can produce systematic errors caused by a spectrum of LETs reaching the sensitive volumes, which affects the cross sections in a way that is very difficult to quantify.

We used a flip-chip 128 Mb SRAM DUT fabricated in IBM's 32 nm SOI CMOS process. The SRAM was originally developed for technology qualification and line monitor purposes. The SRAM is divided into two 64 Mb arrays, which make up the left- and right-hand sides (LHS and RHS) of the chip. Each 64 Mb array consists of sixty-four 1 Mb blocks, where each 1 Mb block is part of a larger 8 Mb block used for data input/output. Within the SRAM there are two cell types, called S262 (LHS) and M234 (RHS), each implemented as one of the 64 Mb arrays. The cell types differ slightly in dimensions and design, where the digits indicate the cell size in 0.*xxx* µm^2 – e.g., 2.34 or 2.62×10^{-9} cm^2/bit. The SRAM was loaded with a variety of data patterns while under test, including blanket and checkerboard variations (logical and physical). The rest of this paper will focus exclusively on the blanket patterns to facilitate a more in-depth analysis of the hardness assurance implications of low-energy proton test methods.

Because of the flip-chip packaging, we had to irradiate the DUT through the substrate, which required mechanical thinning to mitigate particle range limitations. We used an ULTRA TEC ASAP-1 IPS selected area preparation system to thin the SRAM substrate from 760 µm to approximately 100 µm. While processes can be optimized, thickness variation across the die surface is unavoidable when using a mechanical or chemical thinning process that leaves some amount of silicon behind. Silicon is close to the density of aluminum and is a very effective shielding agent – certainly more so than air or Mylar – so it's important to minimize its presence as much as practicable. Furthermore, since the particles are close to or at end-of-range, small substrate thickness variations produce dramatic results – more so than variations upstream. The ultimate thickness variation may be less than ~20 µm, but that is still sufficient to introduce significant non-uniformities in the energies and ranges of the particle beams delivered to the SRAM's sensitive volumes. This straggle increases the beam's energy width and produces uncertainty in the mean and tails of simulated particle energy distributions.

B. Device Under Test Data

Fig. 3 shows heavy ion single-bit upset (SBU) data that were gathered at the Texas A&M University cyclotron facility (TAMU) on the same 128 Mb SRAM DUT. These data were collected as part of the baseline characterization of this device. The high LET cross section is within a factor of two of the

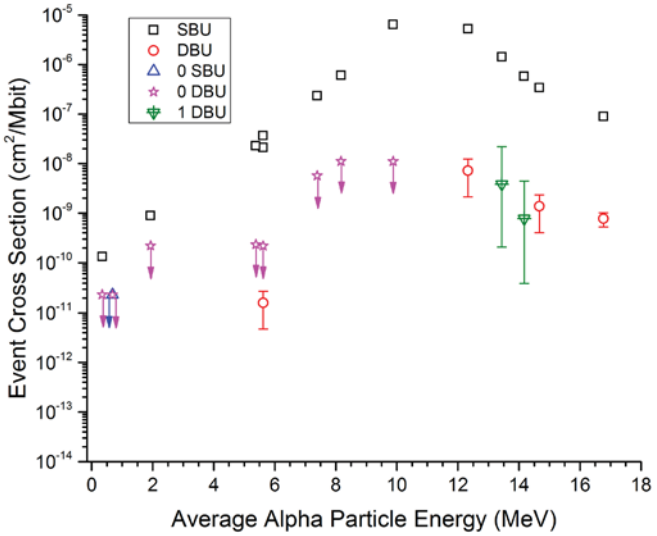

Fig. 4: Alpha particle data on the 0s pattern with an array voltage of 1.05 V (nominal) for the smaller M234 cells. The energies are defined at the device sensitive volume. Limiting cross sections are represented by downward-pointing arrows on the blue triangles and magenta stars. Data points with one event are shown with green triangles. All error bars are 1σ, based on Poisson statistics, with the zero- and one-event limits at the 90% confidence level. If error bars are not shown, they are smaller than the data symbol. All alpha particle energies include beam line and user-controlled degraders, which were calculated using SRIM v2013.

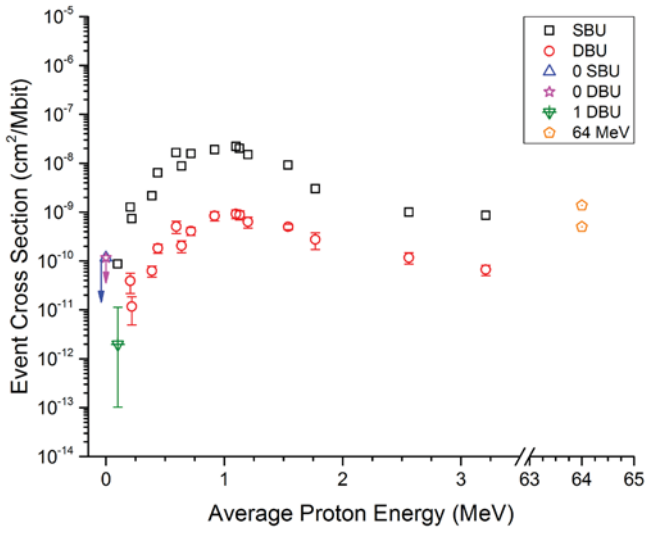

Fig. 5: Proton data on the 0s pattern with an array voltage of 1.05 V (nominal) for the smaller M234 cells. The energies are defined at the device sensitive volume. Limiting cross sections are represented by downward-pointing arrows on the blue triangle and magenta star. Data points with one event are shown with green triangles. All error bars are 1σ, based on the Poisson distribution, with the zero- and one-event limits at the 90% confidence level. If error bars are not shown, they are smaller than the data symbol. For reference, the nominal high-energy proton cross sections are shown. All proton energies include beam line and user-controlled degraders, which were calculated using SRIM v2013.

actual bit cell area and also shows the difference in susceptibility between the S262 and M234 bit cells. The log-log plot highlights the fact that for the large number of events measured (error bars are smaller than the data points) the cross section is not yet saturated, so a higher effective LET may improve bit cell size agreement. Tilt angles were limited to 40 degrees due to package and socket limitations. Data points that look stacked at the same LET are tilt data at 0 and 90 degree roll angles. We present these data as a benefit to the reader and for comparison purposes to the low-energy proton and alpha particle data. Note that these data were collected using a 25 MeV/amu heavy ion beam, which provided a near-constant energy deposition profile through the DUT at the lower LETs. This was not true for the low-energy CNL data where the LET changed rapidly as the ions passed through the silicon.

The data in Figs. 4 and 5 show both alpha particle and proton data on the SRAM DUT for the blanket 0 pattern. All the data were gathered at normal incidence. The data for the M234 cells are broken down into SBU events and double-bit upset (DBU) events. The data sets listed as "0 SBU" and "0 DBU" refer to limiting cross sections where no events were observed – "1 DBU" has an analogous definition. The DBUs represent two physically-adjacent upset bits, which is why the cross section is labeled as events. We observed events with multiplicities up to 4 during testing, but the statistics beyond 2-bit upsets were poor, preventing well-bounded comparisons of these data. Testing at large tilt angles, with roll angle variation, could improve high-multiplicity statistics and/or result in bit upset multiplicities beyond 4. We achieved different alpha particle and proton energies by using various combinations of Mylar and aluminum degrader foils. Note that Figs. 4 and 5 are plotted as a function of average particle energy and do not include horizontal error bars even though each data point represents a range of particle energies. This will be discussed in more detail in the following section.

The alpha particle data in Fig. 4 do not rise above 1×10^{-5} cm^2/Mbit, which would put them within a factor of two of the cross section measured at 1 MeV-cm^2/mg in Fig. 3. However, referring back to Fig. 2, in order to elevate the cross section to that level a large fraction of the degraded alpha particles would have to be close to 1 MeV so that their LETs would be at or above 1 MeV-cm^2/mg. Furthermore, in the case of the alpha particles and protons, we have to contend with the DUT substrate thickness variation and beam energy straggle in ways not present for the heavy ion data. The proton data also include LET distributions much broader than the light ion data, though the issues would be the same as those encountered with the alpha particles.

Many features of these data are consistent with previous reports, including the rise in DBUs at low proton energies, which was first reported in [8]. Despite the relevant comparisons to prior data sets, the data presented here are new in several important ways. First, the low-energy protons and alpha particles were delivered under identical circumstances, enabling comparisons that were previously not possible.

Second, for the multi-bit effects, we gathered limiting cross sections that included particles with kinetic energies placing them at end-of-range for both protons and alpha particles. Low-energy proton measurements in previous studies were also affected by protons with average kinetic energies below

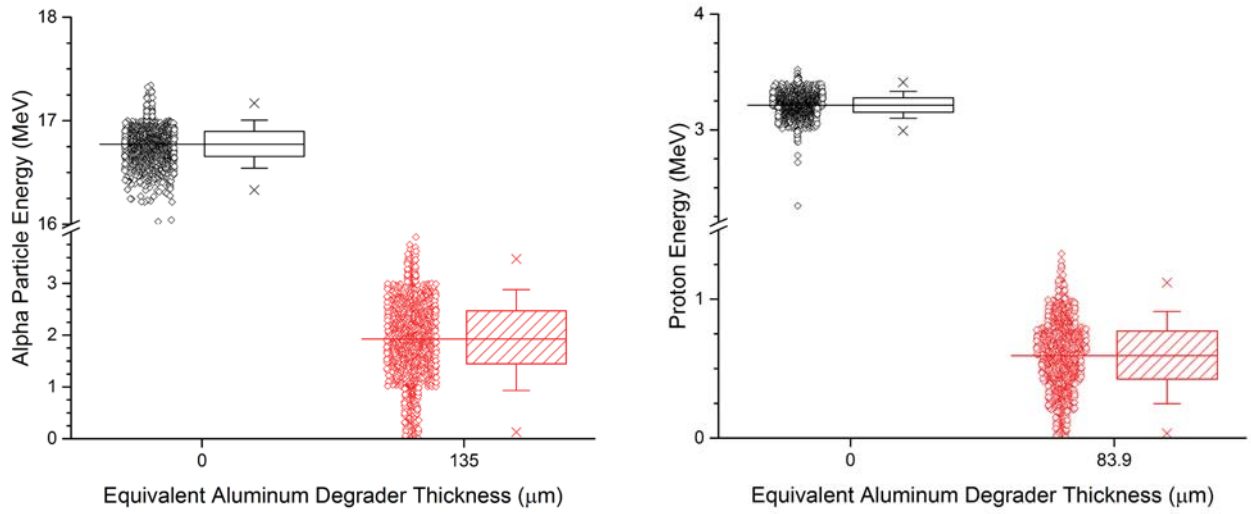

Fig. 6: Box plots showing simulated (a - left) alpha particle and (b - right) proton energy distributions for the baseline beam line configuration with no added degraders as well as a data set close to the Bragg peak where additional degraders were added. The energies are defined at the device sensitive volume. The alpha particles start at 30 MeV and the protons start at 6.5 MeV. The horizontal line shows the mean, the box represents 25% and 75% of the distribution, the whiskers are placed at 10% and 90%, and the "Xs" represents 1% and 99%. These distributions are comprised of 2k events simulated using SRIM v2013. For alpha particles, the 10%-90% energy delta is 0.47 MeV with no degraders and 2.0 MeV with degraders. For protons, the difference is 0.23 MeV and 0.66 MeV. In the lower energy cases, the energy spread is nearly equal to or greater than the mean. Note that the x-axis size of the data clusters does not correspond to a measureable unit – the data are simply grouped for the two categories listed.

1 MeV, because a spectrum of proton energies reaches the sensitive volumes. Data like those of Fig. 5 have a similar shape to those of Fig. 2, but for a very different reason. The cross sections with average proton energies below 1 MeV in Fig. 5 are caused by flux depletion rather than decreasing electronic LET, which is shown in Fig. 2. In this type of experiment, we do not have the capability to deliver monoenergetic beams to the sensitive volumes.

Finally, the real power of these proton and alpha particle data is not their mutually exclusive analysis, but the insights gained by direct comparison, particularly for the MCUs.

C. Conversion of Degrader Thickness to Average Energy

One of the key steps required for this type of single-event effects analysis is the ability to convert the independent variable from degrader thickness to average particle energy. In the early stages of data analysis, it is not uncommon to plot data like those in Figs. 4 and 5 as a function of degrader thickness rather than energy. Completing this conversion step relies on two things: 1) knowledge of the ion beam's initial tune energy, and 2) knowledge of the physical characteristics (composition, density, dimensions, etc.) of all materials that the ion beam intersects. With enough precision and an appropriate radiation transport tool like SRIM, it is possible to accurately convert degrader thickness into an energy distribution. However, gaining enough accuracy and precision to eliminate the dominating systematic errors is not trivial.

In our case, the DUT substrate is the limiting factor for degrader-to-energy conversion. As discussed, we thinned the DUT substrate using a precision mechanical mill. By reducing the substrate thickness, we increased our ability to use lower energy particles for single-event effects testing, but in doing so we also introduced a substantial error source. In the ideal case for an SOI component, we would completely remove the DUT substrate using a chemical process [12, 17, 18], but that approach is not always possible or even desirable. Since a significant amount of substrate is still present, it acts like one of the aluminum degraders further upstream, lowering the beam energy and increasing straggle.

The following procedure assumes that the ion beam will pass through a substantial amount of material, which will be the case when using a relatively high-energy cyclotron accelerator source. Those experiments that employ an electrostatic accelerator and/or a device with little to no substrate will not face these same challenges since the beam energy will be known with a high degree of accuracy due to a tighter initial beam tune and less degrader mass. The combination of an electrostatic accelerator and a device with little or no overburden is the ideal setup for precise energy resolution, but the electrostatic accelerator has limited total kinetic energy compared to other accelerator sources.

We used a cyclotron and had a large amount of material in the beam path, including a DUT with a thick substrate, so the general process for converting from degrader thickness to energy uses the following steps.

1) While gathering low-energy data, collect beam data where the beam is completely stopped. This is usually determined as the point where the beam energy is lowered until the user stops recording upsets. Record these conditions, including beam tune energy and beam line materials (dosimetry apparatus, degraders, DUT, etc.). The beam can be stopped by using a combination of tune energy and user-supplied degraders. If there is a choice, lowering the tune energy is preferred.
2) Using the beam-stopping combination determined in (1), perform radiation transport simulations with a tool like SRIM, excluding the DUT substrate from

the material stack. The goal is to calculate the impinging ion energy distribution at the DUT sensitive volume for all of the irradiation conditions of interest – ion species, ion energy, tilt angle, *etc*.

3) Perform a statistical analysis on the simulation output from (2) and determine the moments of the ion kinetic energy distribution for each of the simulated scenarios in (2). The first three moments – mean, variance, and skewness – the minimum kinetic energy, and the maximum kinetic energy are usually sufficient for most investigations. However, analysis of the simulated energy distributions may require more advanced modeling techniques, like extreme value statistics, depending on the type of information the experimenter is trying to extract.
4) Using either a range table or a Monte Carlo simulation-based binary search, determine the DUT substrate thickness required to stop the particle-energy combination from (3). We tend to prefer the range table approach since it is efficient and because there is already enough systematic error present to limit the accuracy of the Monte Carlo approach.
5) Using the DUT substrate thickness determined in (4), simulate the beam energy characteristics for every beam energy/degrader combination. An example of this is shown in Fig. 6.

In our case, this process yielded a substrate thickness between 70 and 100 µm. 70 µm was the solution for protons and 100 µm was the solution for alpha particles. This 30 µm variance is probably close to the substrate thickness variation, but it is impossible to know for sure without employing destructive physical analysis or a more advanced non-destructive technique like variometric spectroscopy. We could have used the substrate thickness as a fitting parameter in order to better align the energy conversion between protons and alpha particles, but we chose not to break the self-consistency within each data set. At stopping energies, the range of these particles is less than a micron, so even the best thinning procedures will produce systematic errors – except in cases where all the overlaying material is removed.

Fig. 6 shows the output of several SRIM simulations described above in step (5). The energy straggle at low energy increases substantially and this necessarily assumes that the silicon substrate has a uniform thickness. In reality, the substrate thickness varies across the surface of the die, which means that bit cells in different parts of the SRAM will be exposed to different ion energy distributions. This figure also shows how protons with a mean energy of ~0.5 MeV can increase the upset cross section – some of the protons have energies at or below the Bragg peak. At some point the energy variation will be large enough to stop the ions in some areas and let them pass through in others. We attempted to use this feature to select a small subset of SRAM bit cells to analyze thereby eliminating the need to consider thickness variation across the whole SRAM die. However, the thickness variation was not consistent enough to isolate a single region of the SRAM.

Flux depletion, as described above, impacts the computed cross section. At CNL, the beam flux is determined upstream of the DUT, using the secondary electron emission monitors. However, that measured flux may be much lower by the time the beam intersects the SRAM sensitive volumes. If taken into account, this effect would increase the computed single-event cross section by lowering the measured fluence. The low-energy cross section points in Figs. 4 and 5 would be modified in such a way that the roll-off at low energy would either become a monotonic increase or a pseudo plateau. The procedure outlined above can be used to estimate flux depletion simply by computing the ratio of transmitted particles to launched particles. That fraction can then be used to scale the measured fluence. Ultimately, this type of correction will be required in order to perform accurate event rate calculations, but event rates are beyond the scope of this work. The authors would like to point out that there may be other experimental low-energy proton test techniques that do not necessarily require flux depletion analysis – *e.g.*, those that rely on total substrate removal via chemical and/or mechanical techniques.

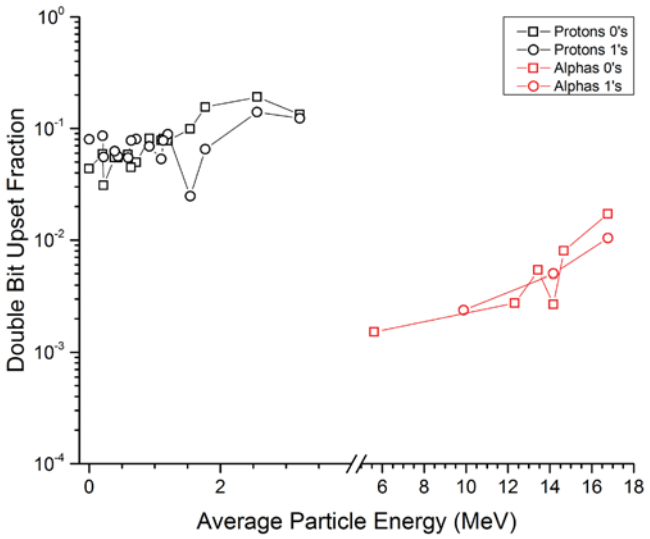

Fig. 7: Comparison of the ratio of the DBU fraction for both alpha particles and low-energy protons. The energies are defined at the device sensitive volume. Both 0s and 1s pattern data are shown. Note that, in this case, we account for the multiplicity of DBU events by multiplying the number of DBU events by 2 before forming the ratio with the number of SBU events. We omitted data points for cases where there were zero measured DBU events.

III. Discussion

The primary point of this work is summarized by the reduced data shown in Fig. 7. Here we see that the fraction of bits involved in DBUs is at least 10x higher for low-energy protons than it is for alpha particles – the difference only increases with decreasing particle energy, approaching nearly 100x at end-of-range. Much of the original low-energy proton work was conducted on larger, albeit still highly-scaled, CMOS technologies. In those cases, the importance of heavy ion MCUs was emphasized and accounted for in experimental practice. However, a combination of mainstream thinking and the physical extent of low-energy proton events kept the issue of low-energy proton MCU in the background. For the 32 nm

process node, and the coming generations of 22 and 14 nm technologies, the device spacing has become small enough that these proton-induced multi-bit events are likely to play a larger role.

As mentioned earlier, Heidel *et al.* [8] presented similar 45 nm SOI CMOS SRAM data with an increasing DBU event cross section as proton energy decreased. That work also alluded to possible mechanisms, since it seemed unlikely that an unperturbed primary proton could cause such a large number of DBUs and other high-multiplicity events. The DBU data we presented also point to an additional implication regarding low-energy proton-induced SBUs. The mechanism responsible for the high-proportion of proton MCUs may also contribute to SBU enhancement, opening the door to further study that may attribute cause to mechanisms beyond primary particle direct ionization. Given what has been presented and published to date, Coulomb scattering could be a possible contributor to both SBU and MCU events.

From an RHA perspective, it is imperative to make an accurate comparison between absolute SBU and DBU cross sections for both protons and alpha particles, which requires accurate knowledge of particle energies. One of the biggest challenges in flip-chip devices is calculating accurate particle kinetic energies inside the silicon body. The mounted devices are not perfectly level to begin with and most thinning procedures still leave variations of at least several microns across the die surface (not bad for an area of ~1 cm^2). These variations are sufficient to cause significant kinetic energy perturbations to the delivered particle beam and ensure that the beam's energy distribution will be smeared further, complicating subsequent analyses.

We feel that additional low-energy proton investigations are needed, particularly those that develop test and evaluation techniques to incorporate low-energy proton single-event effects into the system-level. For example, N. A. Dodds *et al.* [12] have been developing a promising hardness assurance test method separate from, but complementary to, this work. They exploit many of the challenges discussed here, such as beam energy degradation and straggle, in order to develop a nearly closed solution to calculate on-orbit event rates induced by low-energy protons. That type of work coupled with additional mechanism investigations will produce a robust approach to manage low-energy proton single-event effects as technology advances are imposed on our community by the inexorable drive to utilize highly-scaled CMOS devices in the space environment.

IV. Conclusion

Based on the data presented here, we feel that there is likely no suitable proxy for conducting single-event testing with low-energy protons since the multi-bit cross sections measured using protons were higher than those measured with alphas. There are certainly good arguments for skipping low-energy protons if there was a suitable alternative. The testing is difficult and time-consuming, with a lot of experimental variables that require tight control. Furthermore, when using low-energy protons, advanced mechanical or chemical sample preparation techniques are required for many modern technologies due to the use of controlled collapse chip connections. The findings of this work suggest that, despite the rigors, new technologies and designs must be screened with low-energy protons, whether tuned or degraded, to ensure that the low-energy proton sensitivity is well-defined and that RHBD or EDAC techniques are not defeated at the device- or system-level due to higher-than-expected MCU event rates. We are not yet at the point where low-energy proton effects are quantitative at the system level and are faced with evaluating risk and coping with burdensome fault tolerance. In the meantime, studies for event rate calculations that could include low-energy proton effects should use low-energy proton data until the mechanisms responsible for their apparently unique effects are better understood. In the case of older technologies, greater than or equal to the 65 nm process node, it may be possible to use high-energy light ions (e.g., He and N) with a modest amount of risk, but that will depend on a number of factors related to the risk posture of the application and operational system. Low-energy proton single-event effects should loom large for technologies at and below the 45 nm node that are targeted for proton-rich environments such as high-altitude LEO trajectories, trajectories crossing through or operating in Earth's Van Allen Belts or the magnetospheres of other planets, as well as for geostationary and interplanetary systems exposed to unshielded solar particle events.

V. Acknowledgements

The authors wish to thank the staff at the University of California Davis's Crocker Nuclear Laboratory for their dedication to maintaining excellent capabilities for low-energy proton testing. We also want to thank Kevin Stawiasz and Greg Massey of IBM for their technical expertise. Thanks are also due to the many members of the NASA Goddard Space Flight Center Radiation Effects and Analysis Group who provided many good suggestions and stimulating conversation throughout this project.

VI. References

[1] K. P. Rodbell, D. F. Heidel, H. H. K. Tang, M. S. Gordon, P. Oldiges, and C. E. Murray, "Low-Energy Proton-Induced Single-Event-Upsets in 65 nm node, Silicon-on-Insulator, Latches and Memory Cells," *IEEE Trans. Nucl. Sci.,* vol. 54, no. 6, pp. 2474-2479, Dec. 2007.

[2] B. D. Sierawski, J. A. Pellish, R. A. Reed, R. D. Schrimpf, K. M. Warren, R. A. Weller, M. H. Mendenhall, J. D. Black, A. D. Tipton, M. A. Xapsos, R. C. Baumann, D. Xiaowei, M. J. Campola, M. R. Friendlich, H. S. Kim, A. M. Phan, and C. M. Seidleck, "Impact of low-energy proton induced upsets on test methods and rate predictions," *IEEE Trans. Nucl. Sci.,* vol. 56, no. 6, pp. 3085-3092, Dec. 2009.

[3] G. Hubert, S. Duzellier, F. Bezerra, and R. Ecoffet, "MUSCA SEP^3 contributions to investigate the direct ionization proton upset in 65nm technology for space, atmospheric and ground applications," in *European Conf. on Radiation and Its Effects on*

Components and Systems (RADECS), Bruges, Belgium, 2009, pp. 179-186.

[4] E. H. Cannon, M. Cabanas-Holmen, J. Wert, T. Amort, R. Brees, J. Koehn, B. Meaker, and E. Normand, "Heavy Ion, High-Energy, and Low-Energy Proton SEE Sensitivity of 90-nm RHBD SRAMs," *IEEE Trans. Nucl. Sci.,* vol. 57, no. 6, pp. 3493-3499, Dec. 2010.

[5] J. R. Schwank, M. R. Shaneyfelt, V. Ferlet-Cavrois, P. E. Dodd, E. W. Blackmore, J. A. Pellish, K. P. Rodbell, D. F. Heidel, P. W. Marshall, K. A. LaBel, P. M. Gouker, N. Tam, R. Wong, W. Shi-Jie, R. A. Reed, S. M. Dalton, and S. E. Swanson, "Hardness Assurance Testing for Proton Direct Ionization Effects," *IEEE Trans. Nucl. Sci.,* vol. 59, no. 4, pp. 1197-1202, Aug. 2012.

[6] D. F. Heidel, P. W. Marshall, K. A. LaBel, J. R. Schwank, K. P. Rodbell, M. C. Hakey, M. D. Berg, P. E. Dodd, M. R. Friendlich, A. D. Phan, C. M. Seidleck, M. R. Shaneyfelt, and M. A. Xapsos, "Low energy proton single-event upset test results on 65 nm SOI SRAM," *IEEE Trans. Nucl. Sci.,* vol. 55, no. 6, pp. 3394-3400, Dec. 2008.

[7] R. K. Lawrence, J. F. Ross, N. F. Haddad, R. A. Reed, and D. R. Albrecht, "Soft Error Sensitivities in 90 nm Bulk CMOS SRAMs." pp. 123-126.

[8] D. F. Heidel, P. W. Marshall, J. A. Pellish, K. P. Rodbell, K. A. LaBel, J. R. Schwank, S. E. Rauch, M. C. Hakey, M. D. Berg, C. M. Castaneda, P. E. Dodd, M. R. Friendlich, A. D. Phan, C. M. Seidleck, M. R. Shaneyfelt, and M. A. Xapsos, "Single-event upsets and multiple-bit upsets on a 45 nm SOI SRAM," *IEEE Trans. Nucl. Sci.,* vol. 56, no. 6, pp. 3499-3504, Dec. 2009.

[9] N. F. Haddad, A. T. Kelly, R. K. Lawrence, L. Bin, J. C. Rodgers, J. F. Ross, K. M. Warren, R. A. Weller, M. H. Mendenhall, and R. A. Reed, "Incremental Enhancement of SEU Hardened 90 nm CMOS Memory Cell," *IEEE Trans. Nucl. Sci.,* vol. 58, no. 3, pp. 975-980, Jun. 2011.

[10] N. Seifert, B. Gill, J. A. Pellish, P. W. Marshall, and K. A. LaBel, "The Susceptibility of 45 and 32 nm Bulk CMOS Latches to Low-Energy Protons," *IEEE Trans. Nucl. Sci.,* vol. 58, no. 6, pp. 2711-2718, Dec. 2011.

[11] C. Weulersse, F. Miller, D. Alexandrescu, E. Schaefer, and R. Gaillard, "Assessment and comparison of the low energy proton sensitivity in 65nm to 28nm SRAM devices," in *European Conf. on Radiation and Its Effects on Components and Systems (RADECS)*, Sevilla, Spain, 2011, pp. 291-296.

[12] N. A. Dodds, J. R. Schwank, M. R. Shaneyfelt, P. E. Dodd, B. L. Doyle, M. Trinczek, E. W. Blackmore, K. P. Rodbell, M. S. Gordon, R. A. Reed, J. A. Pellish, K. A. LaBel, P. W. Marshall, S. E. Swanson, G. Vizkelethy, and S. Van Deusen, "Hardness Assurance for Proton Direct Ionization-Induced SEEs Using a High-Energy Proton Beam," in *IEEE Nuclear and Space Radiation Effects Conf.*, Paris, France, 2014.

[13] C. M. Castaneda, "Crocker Nuclear Laboratory (CNL) radiation effects measurement and test facility," in *IEEE Radiation Effects Data Workshop*, Vancouver, BC Canada, 2001, pp. 77-81.

[14] J. A. Pellish, P. W. Marshall, C. M. Castaneda, R. A. Weller, D. F. Heidel, K. P. Rodbell, K. A. LaBel, M. D. Berg, H. S. Kim, M. R. Friendlich, A. M. Phan, C. E. Perez, C. M. Seidleck, J. R. Schwank, M. H. Mendenhall, and R. A. Reed, "Low-Energy Proton Testing Using Cyclotron Sources," in *IEEE Nuclear and Space Radiation Effects Conf.*, Las Vegas, NV, 2011.

[15] J. F. Zeigler, and J. P. Biersack. "Stopping and Range of Ions in Matter," http://www.srim.org/.

[16] H. Paul, and A. Schinner, "Judging the reliability of stopping power tables and programs for protons and alpha particles using statistical methods," *Nucl. Instr. and Meth. B,* vol. 227, no. 4, pp. 461-470, 2005.

[17] N. Kanyogoro, S. Buchner, D. McMorrow, H. Hughes, M. S. Liu, A. Hurst, and C. Carpasso, "A New Approach for Single-Event Effects Testing With Heavy Ion and Pulsed-Laser Irradiation: CMOS/SOI SRAM Substrate Removal," *IEEE Trans. Nucl. Sci.,* vol. 57, no. 6, pp. 3414-3418, Dec. 2010.

[18] M. R. Shaneyfelt, J. R. Schwank, P. E. Dodd, J. Stevens, G. Vizkelethy, S. E. Swanson, and S. M. Dalton, "SOI Substrate Removal for SEE Characterization: Techniques and Applications," *IEEE Trans. Nucl. Sci.,* vol. 59, no. 4, pp. 1142-1148, Aug. 2012.